

APPENDIX 4

SEISMIC INDICATORS OF THERMAL AND ROCK PROPERTIES

Table of Contents

1. Vp (P-wave velocity) and Vs (S-wave velocity) Values.....	3
2. Vp/Vs Ratios.....	4
3. Poisson's Ratio.....	6
4. Vp*Vs.....	6
5. Dispersion.....	6
6. Crustal Phase Properties and Correlation with Heat Flow, Temperature, and Rock Composition.....	6
6.1. Pn, Sn Velocity.....	6
6.2. Shear wave splitting (SWS, acoustic birefringence).....	7
6.3. Seismic Noise.....	7
6.4. Seismic Attenuation in the Crust.....	7
7. Density and Seismic Velocity.....	8

LIST OF TABLES

Table A4-1. Summary of results of tomography on magma systems (Lees, 2007).....	10
--	----

1. V_p , V_s values

Although Lees (2007) argues that seismic velocity is a relatively insensitive estimator of temperature variations in rocks, seismic inversion for three-dimensional variations of velocity and attenuation are often used to delineate magma bodies in the crust and upper mantle. Laboratory measurements (Jaya et al., 2010) show that P-wave velocities decrease with increasing temperature in a systematic way (for P-velocity from 1-4 km/s and temperature from 0-300°C), implying that fluid characteristics, with modifications that allow for the presence of bubbles and microfracturing, account for much of the seismic velocity changes.

Lees (2007) summarizes (Table A4-1) tomographic inversions for P-wave and S-wave velocity/attenuation for large calderas, rift zones and smaller scale subduction zone volcanoes. The results vary considerably from place to place, most anomalies are found to be in the range of $\pm 10\%$ seismic velocity perturbation, a range often controlled by the method of smoothing or regularization imposed during inversion. At many volcanoes high velocity anomalies are observed in the shallow regions below magmatic active areas where conduits, dykes or sills are expected to be present. At other locations low velocity perturbations are seen and interpreted as magma accumulation. Most seismic tomography at volcanic regions involves exploring seismic velocity variations and, in some cases, seismic attenuation. Low velocity anomalies below volcanoes were seen at oceanic spreading centers in the east Pacific, Long Valley, Yellowstone, and volcanoes including Rabaul, Krafla, St. Helens, Mt. Rainier, Newberry, Medicine Lake, Unzen, Nikko-Shirane, Fuji, Klyuchevskoy, Campi Flegrei, and Pinatubo. These were interpreted as evidence for melt accumulation in various forms of dykes, sills or magma chambers. While a few examples showed evidence of shallow low velocity associated with active conduits, most low velocity anomalies attributed to melt accumulation lie deeper in the crust, in the range of 8–15 km depth. Lees suggests that, while it is not practiced yet, the combination of inverting for all four seismic parameters (V_p , V_s , Q_p and Q_s) simultaneously may offer a possible way to constrain resulting images and improve resolution.

Unruh et al. (2001) demonstrated that seismic imaging can provide valuable information about the structure of a conventional geothermal field hosted in crystalline (i.e., “transparent”) rocks. Shallow seismic velocity structure estimated from inversion of P-wave first arrival times in the producing areas of the Coso field was relatively lower compared to the non-producing areas. This was explained by localized brittle faulting and hydrothermal alteration. In their study of the central Taupo Volcanic Zone, New Zealand, using local earthquake tomography, Sherburn et al. (2003), could not identify the shallow crustal (down to 6 km depth) basement rocks, however, they observed low V_p anomalies coincident with the location of caldera collapse structures, which they interpret as being associated with low-density volcanoclastic sediments.

Velocities tend to be sensitive to the pore fluid content. Usually the P-wave velocity is most sensitive and the S-wave velocity is less sensitive. Velocities almost always increase with effective pressure. For reservoir rocks they often tend toward a flat, high pressure asymptote. The pressure dependence results from the closing of cracks, flaws, and grain boundaries, which elastically stiffens the rock mineral frame. The only way to know the pressure dependence of

velocities for a particular rock is to measure it in a laboratory. The amount of velocity change with pressure is a measure of the number of cracks; the pressure range needed to reach the high pressure asymptote is a measure of crack shape (e.g. aspect ratio).

While it is generally accepted that seismic velocity depends on the crack density and porosity, it is still not obvious how to translate seismic velocity data into a measure of permeability. Since the permeability is extremely sensitive to the crack width, the permeability of a rock containing fractures of several widths is controlled by a few largest fractures. Thus, a rock with a low density of wide, connected, open cracks and high seismic velocity would still have a high permeability. Seismic velocity and reflectivity are related via porosity to effective stress (Peacock et al., 1997).

A collection of parameters which influence seismic velocity from different regions in the world can be found in Appendix 4a and Appendix 4b.

2. V_p/V_s ratios

In general, V_p and V_s velocities decrease slowly with increasing temperature (Kern, 1982), until they approach the melting point where properties change rapidly. Increases in V_p/V_s ratio are related to increases of temperature, fracture, and especially partial melt (Sanders et al. 1995). Laboratory measurements and theoretical estimates (Mavko, 1980) of seismic wave propagation in the presence of melts show that physical properties vary considerably. Perturbations of seismic velocity due to 10% melt vary only by 10–40% for P-waves and can be 20–100% for S-waves (Iyer and Dawson, 1993). V_p/V_s ratio decreases can be associated with the presence of gas or supercritical fluids.

Fluid saturation generally induces higher P-wave velocity and saturated, unconsolidated sediments typically have high V_p/V_s ratios (Nicholson and Simpson, 1985). Saturation conditions and possibly porosity can thus occasionally be inferred from the comparison of V_p and V_s data (Lees and Wu, 2000). V_p is expected to increase when saturation increases while V_s remains nearly the same, driving V_p/V_s higher (Ito et al., 1979). However, partial melt may decrease V_p and fluid saturated zones will have a net low V_p , low V_s and thus, high V_p/V_s (Walck, 1988).

V_p/V_s ratios are sensitive to phase changes in geothermal systems. Water and steam filled pore spaces affect both P and S wave transmission differently. The ratio of P-wave velocity to the S-wave velocity (V_p/V_s) and Poisson's ratio (σ) are known to be directly related to the rock properties such as compressibility. O'Connell and Budiansky (1982) have shown that a rock's moduli are affected by the degree of water saturation. The velocity ratio (V_p/V_s) increases with pressure increases from vapor saturated (low pore-pressure) conditions to liquid saturated (high pore pressure) conditions (Ito et al., 1979). It is also known that S-waves are more intensely affected by anisotropy than P-waves and that V_p/V_s ratios are expected to vary with azimuth. This is important in delineating geological structures with contrasting physical properties within the reservoir. Such structures are normally important barriers or conduits for fluid flow in the reservoir. Many researchers have investigated how fluid-filled pores in matrix rocks affect seismic wave velocity, and have concluded that the velocity of the matrix rock containing fluids exhibits lower values than that without fluids (e.g. O'Connell and Budiansky,

1974; Mavko, 1980; Schmeling, 1985; Takei, 2002). On the other hand, it has been known that variation in V_p/V_s of matrix rock including fluids depends not only on the kind of fluids but also on the shape of the pores (e.g. Schmeling, 1985; Takei, 2002), which leads to complicated conclusions in interpretations of the causes of seismic velocity anomalies. However, it is certain that melt-filled inclusions result in high V_p/V_s (e.g. Takei, 2002). Nakajima et al. (2001a) discussed the causes of variations in V_p , V_s and V_p/V_s observed in the crust and upper mantle beneath NE Japan, and concluded that low V_p , low V_s and low V_p/V_s in the upper crust are caused by inclusions of H_2O within pores of a relatively large aspect ratio and that low V_p , low V_s and high V_p/V_s in the lower crust and uppermost mantle are caused by melt inclusions.

V_p/V_s variations depending on temperature variations are still ambiguous (e.g. Christensen, 1996) and are difficult to evaluate correctly. For example, the experimental results of Fielitz (1971) imply that V_p/V_s values of rock samples vary with temperature, while Kern and Richter (1981) measured Poisson's ratio of various rocks and concluded that it does not change much with temperature; the average change in Poisson's ratio for rock samples was $\sim 1\%$, within experimental error.

Studies of V_p/V_s ratios have been done in several geothermal fields (McEvilly et al., 1978; Majer and McEvilly, 1979, Foulger et al., 1997, Julian, et al., 1996, 1998). These studies show that water dominated systems such as East Mesa, USA and Cerro Prieto, Mexico have high ratios of 1.55-1.68. These fields were also found to have low reservoir draw down during exploitation. Batini et al. (2010), applying tomography methods at the Larderello geothermal area, found a sharp low velocity zone in the center of the geothermal area, characterized by 15-20% diminished P wave velocity, and associated with a deep low-density body inferred by gravity studies. They have interpreted their results as evidence for an intrusive, still partially molten body that might be the heat source of the area. Steam dominated fields such as The Geysers and Coso Hot Springs, USA have lower ratios, and high reservoir draw down. Low V_p/V_s anomalies at The Geysers are found to correlate reasonably well with regions in the reservoir known or thought to be vapor dominated, consistent with the fluid compressibility mechanism. However, detailed examination of three dimensional inversions of compressional and shear velocities at The Geysers do not seem to support a simple interpretation based solely on variations in fluid compressibility.

There is a negative correlation between V_s and V_p/V_s , along with a notable lack of correlation between V_p and V_p/V_s . These observations (Boitnoit and Kirkpatrick, 1997) are at odds with simple interpretations based on poroelasticity, and suggest that the velocity anomalies reflect processes or phenomena not typically included in interpretations of field seismic data. These authors suggest that shear weakening may influence the properties of field-scale features, or dry reservoir (low pore fluid compressibility) correlates with regions of low pore pressure (depleted reservoir), or the effects of variability in preferred orientation of fractures may also play a role in producing field scale V_p/V_s anomalies. Simiyu (1999) interpreted low Poisson ratio and low V_p/V_s values as be due to high temperature and steam/gas saturation in geothermal fields located in the Kenya rift south west of the Lake Naivasha. A low V_s and low V_p/V_s region relating to the old magma body of volcanoes around of the Otake-Hatchobaru geothermal area in central Kyushu, Japan was located at the depth deeper than 5 km by Yoshikawa and Sudo (2004).

3. Poisson's ratio

Poisson's ratio can be a useful indicator of lithology, pore fluid pressure and compressibility. On average, the Poisson's ratio is 0.25 (representing a "Poisson solid" where Lamé's constant equals the shear modulus) for Earth's crust and upper mantle (Holbrook et al., 1988). Furthermore, there is a strong dependence of Poisson's ratio on the overall volume of cracks and their aspect ratios (Koch, 1992). Poisson's ratio can be computed from V_p/V_s and vice versa.

4. V_p/V_s

This parameter has been used to delineate porosity in sedimentary rocks (Iverson et al., 1989). It has been observed that lower V_p/V_s indicates an increase of porosity whereas V_p/V_s , constant for a specific lithology, does not change with porosity (Pickett, 1963; Tatham, 1982). In geothermal settings, porosity distributions may be more critical for understanding the physics of the field than lithologic variations (Lees and Wu, 2000).

5. Dispersion

Dispersion is the property of acoustic waves of different wavelength to propagate with different velocity. Fluid mobility determines pore-pressure distribution as a fully saturated rock is deformed slightly when a seismic wave passes. Thus, seismic properties are influenced not only by the kind of pore fluid but also by the fluid's ability to move within the rock (Batzle et al., 2006). According to Batzle et al. (2006), with sufficient information, waveform dispersion could be used as a fluid indicator or as a remote measurement of permeability. Dispersion is a complex function of heterogeneity, pore-fluid properties, and mobility.

6. Crustal Phase Properties and Correlation with Heat Flow, Temperature and Rock Composition

6.1 Pn, Sn velocity

In India, Sharma et al (1991) found an inverse relationship among Pn velocity and surface heat flow. Low Pn velocity is associated with elevated temperatures in the upper-most mantle. In the Basin and Range province, Chung (1977) showed that the pronounced low-velocity, low-Q zone and anomalous travel-time delays of both P and S waves are consistent with the combined effects of high temperature, chemical composition, phase changes, and partial melting. The observed low Pn velocity was consistent with high temperature, chemical composition, and the presence of a partially molten layer within the upper mantle, however, the observed teleseismic delay times resulted principally from the thickness of the low velocity zone. Thermal anomalies proposed to have sources in the crust in some areas are consistent with gravity and shear-wave anomalies and support studies in those areas, that suggest high crustal radiogenic concentrations in relatively less dense, granitic crustal rocks (Reiter, 2008).

6.2 Shear wave splitting (SWS, acoustic birefringence)

A single shear-wave propagating through anisotropic rock is split into two orthogonally polarized shear waves, one faster than the other. SWS is higher at low pressure and decreases with the pressure increase. Laboratory seismic measurements performed by Christensen (1978)

have shown that crustal rocks can be strongly anisotropic for shear waves. More recent petrophysical investigations indicate that there is a close relationship between the intrinsic anisotropy (generated by preferred crystal orientations), the birefringence, and the rock structure (foliation and lineation). This relationship may yield information on the crustal structure from shear-wave splitting studies (Barruol and Kern, 1996). Thus, both petrophysical and seismological developments are pointing the way towards use of SWS as a tool to investigate crustal nature and structure.

Malin and Shlev, 1999, developed a method for mapping subsurface fracture density using the time differences of split shear waves from microearthquakes. In regions where a consistent direction of fracturing exists, shear waves from different source and receiver locations are systematically split into fast and slow components. The greater the fracture density, the greater the time differences between the fast and slow components for a given path length. Also, the greater the path length in the fractured rock, the greater the time difference. With a large number of spatially distributed sources and receivers, tomographic back projection of the time differences can be used to map the distribution of fracture density and orientation of the fractures.

To detect the geometry and density of fracture systems at the Coso geothermal field Vlahovic et al. (2002) applied shear-wave splitting to microearthquakes recorded by a permanent, 16-station, downhole, 3-component seismic array running at 480 samples/s. The analysis of shear-wave splitting (seismic birefringence) provided parameters directly related to the strike of the subsurface fractures and their density (number of cracks per unit volume), and, consequently, it is an important technique to outline zones of high permeability. Major fracture directions and orientations were consistent with the known strike of local sets of faults and fractures in local wells and at the surface, as well as with previous analyses of seismic anisotropy in the region.

6.3 Seismic noise

Clearly defined areas of seismic noise at 1.8 km depth have been found by Georgsson et al. (2000), to be associated with the active fracture zone at the eastern flank of the Bakkahlaup field, Iceland, and may partially reflect boiling within the reservoir or partial cracking due to cooling of rocks.

6.4 Seismic attenuation in the crust

Laboratory measurements (Jaya et al, 2010) on two Icelandic geothermal rock samples at simulated in-situ reservoir conditions show that at low temperatures seismic attenuation decreases with temperature due to the rapid decrease in the fluid viscosity. On the other hand, at higher temperatures the attenuation increases because of the generation of bubbles and thermal microfractures.

Laboratory experiments done at high temperature and seismic frequencies (e.g., Kampfmann and Berckhemer, 1985) show that Q_s and Q_p may drop by a factor of 5–10 as temperature increases close to solidus. Heterogeneities within the crust are randomly distributed and occur on a wide range of scales (Frankel and Clayton, 1986; Wu and Aki, 1988; Wu and Flattd, 1990). In the Earth's interior such variations occur at scales down to the grain size of rocks (Holliger et al., 1994). These heterogeneities are due to spatial variations in composition, porosity and

fracturing, and changing conditions in pore pressure, temperature and stress. Wavelength-scale heterogeneity can produce significant seismic scattering and attenuation, and may be of importance in imaging the Earth's interior (Gibson and Levander, 1988; Holliger et al., 1994; Levander et al., 1994).

7. Density and Seismic Velocity

Birch (1961) gave a fundamental empirical relation between density ρ and seismic velocity V_p :

$$\rho = A(M) + BV_p$$

with the constants A and B, of which A is depending on the mean atomic weight M.

Introducing the seismic parameter $F = v_p^2 - 4/3 v_s^2$ Birch's relation was modified by Anderson (1967) who proposed the density/velocity relation of:

$$\rho = AMF^n$$

with the constants A and n. Confining the density/velocity relations to rocks of constant Poisson's ratio and mean atomic weight Knopoff (1967) found a simple density definition of:

$$\rho = Av_p^{2/3}$$

Systematics in the relation between density and seismic velocity on the basis of mineralogical constitution are outlined in detail by Shankland (1977) and Buntebarth (1982).

Table A4-1. (from Lees, 2007)

Table 1
Summary of results of tomography on magma systems

Location	Tectonic style	Volcanic products	Type	Result	Analysis type	Citation
Oceanic Ridge						
East Pacific Rise	Oceanic Ridge	Basalt	Ridge	Small, shallow, low V_p	Marine seismic	Toomey et al. (1990)
Juan De Fuca Ridge	Oceanic Ridge	Basalt	Ridge	Low V_p , 6 km ³ ; 10% melt	Marine seismic	Menke et al. (2002)
Upper Mantle						
Japan	Subduction	Basalt-andesite	Subduction	Numerous low velocity anomalies somewhat correlated to volcanic centers	Subduction seismicity	(Zhao and Hasegawa, 1993; Zhao and Hasegawa, 1993; Iwamori and Zhao, 2000; Zhao et al., 2002)
Kamchatka	Subduction	Basalt-andesite	Subduction	Low velocity somewhat correlated to volcanic centers	Subduction zone eqs	Gorbatov et al. (1999)
Tonga	Back-arc	Basalt-andesite	Subduction	Low V_p	Teleseismic; slab eqs	Zhao et al. (1997)
Cascadia	Subduction	Basalt-andesite	Subduction	Low velocity, low Q_p , correlated to volcanic centers	Regional eqs	Lees and Crosson (1990)
Andes	Subduction	Basalt-andesite	Subduction	Low velocity somewhat correlated to volcanic centers	Teleseismic	Schurr et al. (2003)
Calderas						
Long Valley	Rift	Rhyolite	Caldera	Large small amplitude anomalies associated with the caldera; Low Q_p , Q_s anomalies	Teleseismic and local	(Peppin, 1985; Dawson et al., 1987; Hauksson, 1988; Dawson et al., 1990; Sanders, 1993a,b; Sanders et al., 1994; Steck, 1995; Sanders et al., 1995; Weiland et al., 1995; O'Doherty et al., 1997)
Yellowstone	Hot Spot	Rhyolite-basalt	Caldera	Low V_p , V_s 1-3% anomaly; low Q_p	Teleseismic	(Iyer et al., 1981; Benz and Smith, 1984; Clawson et al., 1989; Miller and Smith, 1999; Husen and Smith, 2004; Yuan and Dueker, 2005)
Valles	Rift	Rhyolite	Caldera	Shallow low velocity; deep low V_p 12-15 km depth	Teleseismic	Lutter et al. (1995)
Taupo	Subduction	Dacite	Caldera	No clear low velocity anomaly		Sherburn et al. (2003)
Rabaul	Subduction	Basalt-andesite-dacite	Pyroclastic shield	Low V_p 3-6 km depth	Local	Finlayson et al. (2003)
Toba	Subduction	Basalt-dacite	Caldera	Low velocity 37%	Local	Masturyono et al. (2001)
Iceland						
Krafla	Rift	Basalt	Caldera	Shallow low velocity	Local	(Einarsson, 1978; Foulger and Amott, 1993)
Hekla	Rift	Basalt	Stratovolcano	No significant anomalies	Local	Soosalu and Einarsson (2004)
Torfbjökull	Rift	Basalt	Stratovolcano	No significant anomalies	Local	Soosalu and Einarsson (2004)
Hengill-Grensadalur	Rift	Basalt	Crater rows	10% low velocity	Local	Toomey and Foulger (1989)
Cascadia						
Newberry volcano	Subduction	Basalt-rhyolite	Shield volcano	Low V_p < 10%	Local; synthetic	(Achauer et al., 1988; Stauber et al., 1988)
Medicine Lake	Subduction	Basalt-rhyolite	Shield volcano	Low V_p < 10%	Local; active source	(Evans and Zucca, 1988; Lees and Crosson, 1989; Ritter and Evans, 1997)

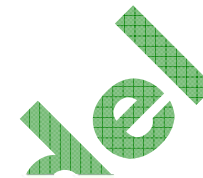


Table 1 (continued)

Location	Tectonic style	Volcanic products	Type	Result	Analysis type	Citation
Cascadia						
Mt. St. Helens	Subduction	Andesite–dacite and occasional rhyolite	Stratovolcano	High V_p 20% top of stoping zone; Low V_p conduit and deep Low V_p	Local earthquake	Lees (1992)
Mt. Rainier	Subduction	Granodiorite–andesite	Stratovolcano	Low V_p 8–15 km	Local–regional eqs	(Lees and Crosson, 1990; Moran et al., 1999)
Alaska						
Redoubt	Subduction	Basalt–dacite	Stratovolcano	10% perturbations; no clear magma body	Local eqs	Benz et al. (1996)
Japan						
Unzen	Rift	Basaltic	Complex volcano	Low V_p	Local–regional eqs	Ohmi and Lees (1995)
Onikobe	Subduction	Basalt–dacite	Volcanic chain	Low V_p , V_s , high V_p/V_s	Local eqs	Nakajima and Hasegawa (2003)
Kirishima	Subduction	Basalt–dacite	Shield volcano	High and low velocity; low Q	Local–regional eqs	Yamamoto and Ida (1994)
Nikko-Shirane	Subduction	Basalt–dacite	Shield volcano	30% low V_p 5–15 km depth	Local eqs	Horiuchi et al. (1997)
Mt. Fuji	Subduction	Basalt–dacite	Stratovolcano	Low V_p below summit	Local–regional eqs	Nakamichi (2005)
Kamchatka						
Klyuchevskoy	Subduction	Basalt–dacite	Stratovolcano	Low V_p 25–40 km depth	Local–regional eqs	(Anosov et al., 1978; Ozerov, 2000)
Hawaii						
Halemaumau	Hot Spot	Basalt	Shield	Low V_p 6 km deep	Local eqs	Rowan and Clayton (1993)
Kilauea	Hot Spot	Basalt	Shield volcano	Low V_p , High V_p in shallow conduit	Local eqs	(Thurber, 1984; Rowan and Clayton, 1993; Okubo et al., 1997; Haslinger et al., 2001)
Italy						
Vesuvius	Subduction	Basalt–dacite	Somma volcano	No shallow anomaly; Low V_p at 8 km depth	Local eqs	(De Natale et al., 1998; Zollo et al., 1998)
Campi Flegrei	Subduction	Basalt–dacite	Caldera	Low velocity 3–4 km; gas accumulation?	Local eqs	1988; Aster et al., 1992
Mt. Etna	Subduction	Basalt–dacite	Stratovolcanoes	High velocity	Local eqs	(Cardaci et al., 1993; Villaseñor et al., 1998; Laigle and Hirn, 1999; Chiarabba et al., 2000; Aloisi et al., 2002)
Indonesia						
Pinatubo	Subduction	Basalt–dacite	Stratovolcano	Low V_p 6–11 km depth; 15% anomaly	Local eqs	Mori et al. (1996)
S. America						
Nevado del Ruiz	Subduction	Basalt–dacite	Stratovolcano	Low V_p and V_s	Local eqs	Londoño and Sudo (2003)
Tungurahua	Subduction	Andesitic	Stratovolcano	High V_p in upper 4–5 km	Local eqs	Molina et al. (2005)
Canary Islands						
Gran Canaria	Hot spot	Basaltic	Fissure vents	No low velocity	Local eqs	Krastel and Schmincke (2002)

